Geochimica et Cosmochimica Acta
February 2019, Volume 246, Pages 450-460
https://doi.org/10.1016/j.gca.2018.12.009
https://archimer.ifremer.fr/doc/00472/58335/

Zinc isotopic variations in ureilites

Brugier Yann-Aurélien [1], Barrat Jean-Alix [1, *], Gueguen Bleuenn [2], Agranier Arnaud [1], Yamaguchi Akira [3, 4], Bischoff Addi [5]

[1] Laboratoire Géosciences Océan (UMR CNRS 6538), Université de Bretagne Occidentale et Institut Universitaire Européen de la Mer, Place Nicolas Copernic, 29280 Plouzané, France
[2] UMS CNRS 3113, Université de Bretagne Occidentale et Institut Universitaire Européen de la Mer, Place Nicolas Copernic, 29280 Plouzané, France
[3] National Institute of Polar Research, Tachikawa, Tokyo 190-8518, Japan
[4] Department of Polar Science, School of Multidisciplinary Science, SOKENDAI (the Graduate University for Advanced Studies), Tokyo 190-8518, Japan
[5] Institut für Planetologie, Westfälische Wilhelms-Universität Münster, Wilhelm-Klemm-Str. 10, 48149 Münster, Germany

* Corresponding author : Jean-Alix Barrat, email address : barrat@univ-brest.fr

Abstract :

The Ureilite Parent Body (UPB) was a C-rich planetary embryo disrupted by impact. Ureilites are fragments of the UPB mantle and among the most numerous achondrites. Zinc isotopic data are presented for 26 unbrecciated ureilites and a trachyandesite (ALM-A) from the same parent body. The δ66Zn values of ureilites range from 0.40 to 2.71 ‰ including literature results. Zinc isotopic compositions do not correlate with the compositions of olivine cores, with C and O isotopic compositions, with Zn abundances, nor with shock grades. The wide range of δ66Zn displayed by the ureilites is chiefly explained by evaporation processes that took place during the catastrophic breakup of the UPB. During breakup, the high temperatures of the UPB mantle allowed Zn to evaporate, regardless of the intensity the shock suffered by the ureilitic debris. For the most shocked of them, post-shock heating permitted greater evaporation, and heavier Zn isotopic compositions. The surface of the UPB was certainly much colder than the mantle before the breakup. Therefore, crustal rocks were probably less prone to Zn evaporation. ALM-A, the sole crustal rock analyzed at present, has a δ66Zn value (0.67 ‰) significantly higher than those of regular chondrites. This result indicates that its mantle source displayed already non-chondritic Zn isotopic compositions before the breakup of the UPB.

Keywords : ureilite, zinc isotopic composition, isotope fractionation, shock

1. Introduction

Numerous planetesimals and planetary embryos were formed during the first few million years of the solar system, with many of them melting and differentiating into a metal core, an ultramafic mantle and an evolved crust (e.g., Yin et al., 2002; Morbidelli et al., 2012). Today, most of these early bodies no longer exist, being accreted as the building blocks of the rocky planets. However, some of their debris are still present in the asteroid belt, between the orbits of Mars and Jupiter, and sometimes fall on Earth. Petrological and geochemical studies of these meteorites, the achondrites and irons, make it possible to directly address the processes of differentiation of these early-formed bodies. Represented by more than 400 known meteorites, ureilites are one of the main achondrite groups (Yamaguchi et al, 2017). They originate from a now destroyed, single parent body (Downes et al., 2008), the Ureilite Parent Body (UPB). The original size of the UPB is the subject of intense discussions. For some scientists, its diameter was about 200 km (e.g., Wilson et al., 2008). For others, this object was a large planetary embryo with a diameter of at least 690 km (Warren and Huber, 2006; Warren, 2012; Barrat et al., 2017), and may have been much larger, possibly the size of Mars (Nabiei et al., 2018).

The UPB accreted from materials displaying distinctive chemical and isotopic features. Clayton and Mayeda (1988, 1996) have shown that the O isotopic composition of ureilites straddles the CCAM line, with a variation similar to that of CV, CO, and many CM carbonaceous chondrites. Thus, they suggested that the UPB formed from similar primitive materials. This interpretation was unanimously accepted, until, using the systematics of Cr and Ti isotopes coupled with O isotopes, it was demonstrated that ureilites have more affinities with non-carbonaceous materials (Warren, 2011). Recent studies investigating Tm anomalies (Barrat et al., 2016a) and Mo isotopics (Budde et al., 2017) confirm the affinities of the UPB with inner Solar System materials. The UPB accreted during the first 2 My after initial Solar System formation (Budde et al., 2015; Van Kooten et al., 2017) and was heated by decay of short-lived isotopes such as ^{26}Al. This heating triggered the segregation of a S-rich core before the onset of silicate melting (Warren et al., 2006; Rankenburg et al., 2008; Barrat et al., 2015) and a subsequent differentiation event that occurred between 3 and 7 Myr (Goodrich et al., 2010; Bischoff et al., 2014; Budde et al., 2015). Differentiation led to the formation of a crust, by extraction of silica-rich melts (e.g., Bischoff et al., 2014; Barrat et al., 2016b). A major impact with another large planetary embryo at approximately 7 Ma after CAI formation, or later, stopped the differentiation of the UPB, and catastrophically disrupted it (e.g., Goodrich et al., 2015).

A portion of the UPB fragments re-accreted and were mixed with other extraterrestrial materials to form second generation bodies. The bodies survived until final impact-induced ejection of materials to deliver brecciated meteoroids that entered the Earth atmosphere. Indications for these processes are found in ureilitic breccias (Downes et al., 2008), which can be highly polymict as

indicated by the products provided by the Asteroid 2008 TC_3-Almahata Sitta event (Bischoff et al., 2010, Horstmann and Bischoff, 2014, Goodrich et al., 2014a).

The diversity of the accreted materials that formed the UPB, and the complex processes involved in its mantle, are recorded by the ureilites. Most of these rocks are unbrecciated coarse-grained peridotites (grain size usually about 1-3 mm), consisting chiefly of olivine and pyroxene (pigeonite, and more rarely augite and orthopyroxene), abundant carbon (up to 7 wt%, graphite and diamond), with accessory metal and sulfides (e.g., Mittlefehldt et al., 1998). These rocks are mantle restites formed after the extraction of sulfide-rich metallic melts that formed the core of the body, and a variety of magmas that formed a crust (e.g., Takeda, 1987; Scott et al., 1993; Warren et al., 2006; Rankenburg et al., 2008; Bischoff et al., 2014; Barrat et al., 2015, 2016b). These restites display not only a huge diversity in terms of their modal proportions of olivine and pyroxene (they range from dunites to olivine-free pyroxenites), but also in the compositions of the phases (e.g., the olivine cores in any unbrecciated ureilite are uniform, but between samples range from $Fo_{74.7}$ to $Fo_{96.8}$). Furthermore, the compositions of the olivine and pigeonite cores (e.g., Fe/Mn ratios and Mg-numbers (=100 Mg/(Mg+Fe), atomic)), O (Clayton and Mayeda, 1988, 1996) and C isotopic compositions of the rocks are strongly correlated, and indicate the involvement of two reservoirs with distinctive chemical and isotopic features (Barrat et al., 2017). These mantle heterogeneities are probably inherited from the accretion of the body [possibly the merging of two planetesimals as originally evoked by Sanders et al. (2017)].

The breakup of the UPB is well recorded by the mineralogy of the ureilites. Firstly, many ureilites (but not all) were strongly shocked during this event, and display impact diamonds and sometimes mosaicised olivines (e.g., Mittlefehldt et al., 1998; Bischoff et al., 1999). Secondly, all the ureilites exhibit olivines with distinctive Fe-depleted rims and veins produced by localized reduction reactions with C-phases during this event (e.g., Miyamoto et al., 1985; 1993; Warren and Huber, 2006). The lack of large exsolutions in pigeonites demonstrates that ureilites were first equilibrated at temperatures higher than 1200°C. Diffusion calculations performed on the Fe-depleted rims of the olivine crystals point to a sudden transition to a fast cooling (e.g., Miyamoto et al., 1985, 1993). This distinctive step-wise cooling history of the fragments of the UPB's mantle is consistent with a cataclysmic impact, while the mantle of the body was still hot (e.g., Takeda et al., 1987; Warren and Kallemeyn, 1992; Scott et al., 1993; Goodrich et al., 2004).

Since the mid-seventies, it has been shown that heated rock powders and chips under vacuum lose some of their volatile elements by evaporation, notably Zn (e.g., Ikramuddin, 1977a, 1977b; Wulf et al., 1995). Zinc is a moderately volatile element in the solar nebula (Tc=726 K, Lodders, 2003) that displays both chalcophile and lithophile behavior, and has five stable isotopes [^{64}Zn (49.17%), ^{66}Zn (27.73%), ^{67}Zn (4.04%), ^{68}Zn (18.45%), and ^{70}Zn (0.61%)]. Zinc is sensitive to evaporation-

condensation processes and provides promising insights into the origin of volatile element depletions in both primitive and differentiated materials (e.g., Luck et al., 2005; Paniello et al., 2012a, 2012b; Pringle et al., 2017; Mahan et al., 2018 and references therein). Zinc isotopic compositions were previously determined by Moynier et al. (2010) for eleven ureilites. A substantial range of δ^{66}Zn values (≈ 0.6 ‰) was observed. Because these isotopic compositions are inversely correlated with the Zn abundances and because the most shocked samples display the highest δ^{66}Zn values, these authors ascribed the variations to evaporation of Zn upon impacts. Here, we return to this issue with a comprehensive suite of samples covering the whole range of compositions known for unbrecciated ureilites (e.g., with olivine cores ranging from $Fo_{74.7}$ to $Fo_{96.8}$) and a sample of trachyandesitic lava. Our aim was to determine the full range of Zn isotopic compositions for ureilites, but also to discuss the observations made by Moynier et al. (2010). Ureilites are the most comprehensive sampling of an extraterrestrial mantle available on Earth. Therefore, another important objective of this work was to assess the behavior of Zn during the differentiation and the destruction of the UPB.

2. Samples and analytical procedures

We analyzed 27 meteoritic samples. Their main features, including their shock level when known (e.g., Goodrich, 1992), are summarized in Table 1. Twenty-five are typical unbrecciated ureilites found in Antarctica or in Sahara. They are among the least weathered ureilitic finds. Their olivine cores cover the full range of compositions known for ureilites, from $Fo_{74.7}$ to $Fo_{96.8}$. Two other samples were selected: MET 01085, an ureilitic pyroxenite devoid of olivine, and ALM-A, a trachyandesitic stone from the Almahata Sitta fall (Bischoff et al., 2014). Polymict ureilites have deliberately been excluded from our sampling, as have samples of the rare "Hughes" ureilites. Most of the selected samples have been extensively studied. We have already determined the trace element abundances (Bischoff et al., 2014; Barrat et al., 2016a and b), the Fe isotopic compositions (Barrat et al., 2015), and the C isotopic compositions (Barrat et al., 2017) for many of them.

Samples (0.25-1 g) were powdered using a boron-carbide mortar and pestle. About 250 mg of powder for each sample was digested on a hot plate heated to 125°C, using sequential mixtures of HF/HNO_3, HNO_3 and HCl. This procedure ensures a perfect dissolution of all the phases, except graphite and diamond which are devoid of Zn, and possibly chromite. However, the issue of spinel dissolution does not arise here, because our samples are devoid of chromite, or contain just minute amounts of this phase (e.g., LAP 03587, Goodrich et al., 2014b).

For the samples not analyzed for trace element abundances by Barrat et al. (2016b), elemental compositions were determined using a HR-ICP-MS Thermo Scientific Element 2 at PSO (Pôle Spectrométrie Océan (PSO), Ifremer/IUEM/IRD, Plouzané, France), following the same procedure.

About 1 µg of Zn for each sample was purified using an ion-exchange chromatography method adapted from Maréchal et al (1999). The samples were loaded in 6 N HCl in polypropylene columns filled with 2 ml of macroporous AG MP-1 resin. The matrix was eluted in 6 N, 2 N, and 0.24 N HCl and Zn was collected in 0.012 N HCl. Eluted solutions were evaporated to dryness and residues were dissolved in 0.5 N HNO_3. The yield was better than 99 %. The procedural blank was < 6 ng and insignificant relative to the amount of processed Zn.

Isotopic compositions were measured on a Thermo Scientific Neptune multi collector - inductively coupled plasma- mass spectrometer at PSO, using a Cu-doping method (Cu NIST SRM 3114) for correction of instrumental mass bias (Maréchal et al., 1999). Samples were introduced using a cyclonic spray chamber and were analyzed in low resolution mode. ^{63}Cu, ^{64}Zn, ^{65}Cu, ^{66}Zn, ^{67}Zn, ^{68}Zn were collected in faraday cups and ^{62}Ni was collected to monitor potential interferences of ^{64}Ni on ^{64}Zn. Samples and standards were prepared to match a concentration of 200 ppb for Zn and 100 ppb for Cu and ~8 V were measured for ^{63}Cu and ~4.4 V for ^{64}Zn. A standard-sample-bracketing method was employed by measuring the isotopic standard Zn IRMM 3702 doped with Cu NIST SRM 3114 before and after each sample. Zinc isotopes are reported relative to IRMM 3702 using the conventional δ-notation:

$$\delta^{x}\mathrm{Zn}(‰) = 1000\,[(\frac{^{x}Zn}{^{64}Zn})_{sample}/(\frac{^{x}Zn}{^{64}Zn})_{IRMM3702} - 1] \text{ with x=66 or 68} \qquad (1)$$

Previous studies used a different standard [JMC 3-0749C (Lyon standard)]. For the sake of consistency with previous results, we will discuss below the Zn isotopic variations relative to the Lyon standard. $\delta^{66}Zn_{Lyon}$ values are calculated using equation (2), in agreement with the compositions obtained by Sossi et al. (2015) on both standards:

$$\delta^{66}\mathrm{Zn}_{\mathrm{Lyon}}\,(‰) = \delta^{66}\mathrm{Zn}_{\mathrm{IRMM3702}} + 0.30 \qquad (2)$$

Each sample solution was analyzed twice, and the averages are given in Table 1. Our calibration was checked with the USGS standard BHVO-2 basalt for which four aliquots were processed with four different columns, and analyzed twice. The average of the eight analyses (δ^{66}Zn = 0.33 ‰, Table 1) are in excellent agreement with previous studies [e.g., δ^{66}Zn = 0.27 ‰, Sossi et al. (2015), δ^{66}Zn = 0.35 ‰, Doucet et al. (2016), δ^{66}Zn = 0.30 ‰, Pringle et al. (2017) and Huang et al. (2018)]. Moreover, these results illustrate our external precisions (2σ) which are better than 0.05 ‰ for δ^{66}Zn and 0.10 ‰ for δ^{68}Zn. In the following, all the Zn isotope compositions are reported relative to the Lyon standard in the text and figures.

3. Results

The measurements of Zn isotopic compositions, Zn, Ca, and Mn abundances for all of the samples are reported in Table 1. Including previous samples analyzed in Brest (Barrat et al., 2016b), Zn abundances in ureilites range from 89 to 285 µg/g, in agreement with literature data [see Warren et al. (2006) and references therein].

In a δ^{68}Zn vs. δ^{66}Zn plot (not shown), all the samples define a mass dependent fractionation line of slope 2.084 (R=0.9961). The δ^{66}Zn values range from 0.57 to 2.71 ‰. If we set aside ALH 81101, which is one of the most strongly shocked ureilites analyzed in this study, the range is much more restricted, from 0.57 to 1.26 ‰, and similar to the results obtained by Moynier et al. (2010), from 0.38 to 1.04 ‰.

4. Discussion

4.1. Zn abundances and δ^{66}Zn in ureilites

Ureilites display high Zn abundances [89 to 285 µg/g (Table 1), and the highest concentrations (360 µg/g) have been obtained by Warren et al. (2006) in LEW 88006]. The highest concentrations are higher than those in CI or in EH3 chondrites (e.g., Wasson and Kallemeyn, 1988; Rubin et al., 2009), which are the chondrites with the highest Zn abundances. The average ureilite Zn abundance (188 µg/g, n=25, this study) is similar to the average CM abundance, and the lowest abundances in ureilites are still high and on the order of those measured in CO and CV chondrites (e.g., Wasson and Kallemeyn, 1988). Ureilites are much richer in Zn than ordinary chondrites and the primitive terrestrial mantle (Zn= 55 µg/g, McDonough and Sun, 1995). Their high Zn concentrations strengthen the view that they formed from unusually volatile-rich primitive materials, distinct from currently known carboneous chondrites (e.g., Warren et al., 2011).

Rare ureilites have chromite that contain ≈ 400 to 4900 µg/g Zn (Chikami et al., 1997; Goodrich et al., 2014b; Bischoff et al., 2016, Rozén et al., 2019). This phase is certainly a major carrier of Zn for some samples, such as LEW 88774, but chromite-bearing ureilites are exceptional. The vast majority of the ureilites do not contain chromite, nor other "Zn-rich" phases. Zn abundances in ureilitic metal (<70 µg/g) and sulfides (< 10 µg/g) are low compared to whole rock abundances

(Goodrich et al., 2013). The leaching experiments performed by Barrat et al. (2016b) confirm these analyses and show that Zn is not removed from the powders by cold HNO_3, contrary to Cu which is certainly partly hosted by sulfides (Fig.1). These data suggest that the main carriers of Zn in ureilites are more likely olivines and pyroxenes. However, the few in-situ silicate analyses obtained by Goodrich et al. (2013) are surprisingly low (<70 µg/g) and not consistent with the abundances in the whole rocks and in the residues. Two hypotheses can explain this mismatch. Firstly, Zn-rich chromites, that are too small to be detected by routine examination, could be ubiquitous in ureilites. Alternatively, and more probably, the Zn abundances obtained by Goodrich et al. (2013) by LA-ICPMS, are probably underestimated. If not confirmed by additional work, these analyses should be treated with caution. Whether Zn is controlled by chromite, or more likely by silicates, rather than by sulfides and metal that are often oxidized in ureilitic finds is important. It indicates that Zn abundances and isotopic compositions are not sensitive to terrestrial weathering, unless silicates are also altered. This is not the case for the meteorites we have selected here, and the compositions we have obtained are certainly pristine.

Zn isotopic compositions in ureilites are compared to those of major chondritic groups in Figure 2. With the exception of a few samples with an intricate thermal history [e.g., the EL6 (Moynier et al., 2011), and thermally metamorphosed carbonaceous chondrites (Mahan et al., 2018)], the δ^{66}Zn values measured in carbonaceous and enstatite chondrites range from 0 to 0.6 ‰. Ordinary chondrites show much more variations (δ^{66}Zn from -0.5 to 0.8 ‰), but only one of them (Julesburg, a L3.6) shows values higher than 0.55 ‰ (Luck et al., 2005). Ureilites, on the other hand, have very different Zn isotopic compositions compared to regular chondrites. A few have δ^{66}Zn similar to CI chondrites, but most of them display significantly heavier compositions. Moreover, an apparent correlation between Zn abundances and isotopic compositions (r=-0.89) was also obtained by Moynier et al. (2010) with eleven ureilites, with the samples richest in Zn having δ^{66}Zn values closest to CI chondrites, and the poorest showing the heaviest isotopic compositions (Fig. 3). This relationship led these authors to conclude that ureilites initially had Zn abundances and isotopic compositions similar to CIs and that the observed isotopic fractionations were chiefly the result of evaporation during heating events, possibly impacts. Our analyses obtained on a much larger set of samples, do not confirm this trend. The spread of the data in the δ^{66}Zn vs. Zn plot (Fig. 3) points to a much more complex situation. Of course, it is possible that at least part of the dispersion is explained by this process: ALH 81101, one of the most shocked ureilites, displays the highest δ^{66}Zn value. However, the data spread suggests that the effects of other parameters (e.g., heterogeneity of the parent body) or processes (e.g., partial melting) on δ^{66}Zn values should be evaluated in addition to the effects from losses of Zn by evaporation subsequent to the breakup of the UPB.

4.2. Zn in ureilites before the breakup of the UPB

The heterogeneity of the UPB is well illustrated by the diversity of ureilitic olivine core compositions (e.g., Goodrich, 1992; Downes et al., 2008, among others), and by O and C isotopic variations, both of which are well correlated to olivine compositions (Clayton and Mayeda, 1988, 1996; Barrat et al., 2017). Oxygen and C isotopic variation indicates that the wide range of Fe/Mg ratios displayed by ureilites is explained by mixing of two endmembers with contrasting isotopic compositions (Fig. 4a,b). Figure 4c displays the δ^{66}Zn values of ureilites as a function of olivine core compositions. Unlike O and C isotopes, no mixing relationship is obvious with Zn isotopes. Both endmembers were probably characterized by similar δ^{66}Zn values $\geq$ 0.5 ‰, but their isotopic compositions cannot be very precisely constrained with this diagram, not only due to the spread of the data, but also because Zn isotopic compositions could have been largely affected by other processes following the mixing event.

Core formation processes cannot produce resolvable Zn metal-silicate isotopic fractionation (Bridgestock et al., 2014; Mahan et al., 2017), and can be ignored here.

Some recent studies on terrestrial peridotites have suggested that partial melting is able to fractionate Zn isotopes (Doucet et al., 2016; Wang et al., 2017). The most refractory harzburgites have δ^{66}Zn values about 0.2 ‰ lower than fertile lherzolites. Inter-mineral Zn isotope fractionations between clinopyroxene, orthopyroxene, and olivine measured by Wang et al. (2017) in unmetasomatized peridotites, are close to zero within analytical uncertainties. However, spinel displays δ^{66}Zn values heavier than those of coexisting olivine or pyroxenes by ca. 0.1 ‰. Calculations made by these authors show that the lighter Zn isotopic compositions displayed by restitic harzburgites could be explained by spinel-consumption during partial melting. Sossi et al. (2018) and Huang et al. (2018) challenged this interpretation. Sossi et al. (2018) calculated that partial melting is ineffective in producing Zn isotope fractionation in the mantle. Based on analyses obtained on komatiites, the effect of garnet seems negligible too (Sossi et al., 2018). The same conclusion can be made for plagioclase, because this mineral is particularly poor in Zn, and has a totally insignificant contribution to the budget of this element in peridotites. Therefore, Zn isotopes are not significantly fractionated during partial melting of spinel-free plagioclase-bearing peridotites.

The possibility that the UPB was up to Mars-sized in diameter means that it is possible that a number of distinct mineral assemblages were present in its mantle. Most ureilites are devoid of aluminous phases, which have been exhausted during the early stages of partial melting. The fact that a few ureilites display large chromite crystals (e. g., Goodrich et al., 2014b) could suggest that their precursors initially contained Cr-rich spinel. However, if this was the case, the exhaustion of spinel during melting would have considerably depleted ureilites in Cr. Instead, Cr abundances in these rocks are high (≈3200-5000 µg/g, Warren et al., 2006), and similar or higher than the abundances in

chondrites (e.g., Wasson and Kallemeyn, 1988). Therefore, precursors of most known ureilites were likely devoid of spinel. Rare earth elements (including Eu) show that ureilites are restites after more than 15 % partial melting from a chondritic plagioclase-bearing source (Barrat et al., 2016b). Thus, the effects of partial melting on their Zn isotopic compositions was certainly minimal if not negligible.

Figure 5 shows the abundances of Mn and Zn, and the δ^{66}Zn values as a function of CaO abundance. Calcium concentrations were chosen as a parameter for the progress of partial melting: the less calcium in a ureilite, the more residual it is. Manganese is much less volatile than Zn (see O'Neil and Palme, 2008). Both elements have similar partition coefficients for olivine and pyroxenes, and therefore have the same behavior during partial melting (Le Roux et al., 2010). In this diagram, Mn concentrations span a limited range and roughly define a trend in agreement with a slightly incompatible behavior for this element.

Zinc concentrations and isotopic compositions have wide dispersions, and cannot be linked to a simple trend of partial melting. Two hypotheses may explain these spreads. First, the precursors of ureilites were heterogeneous in terms of both the abundance and isotopic composition of Zn. Second, the abundances and isotopic compositions of Zn were significantly modified during the destruction of the parent body. These two possibilities are obviously not exclusive and will be discussed below.

4.3. Zinc in ureilites during the breakup of the UPB

Impact heating is often thought to be the cause of the volatile element depletions seen in the most shocked materials. Indeed, this interpretation seems robust for many chondrites displaying very low Zn abundances and high to very high δ^{66}Zn values (e.g., Moynier et al., 2011; Mahan et al., 2018). However, this conclusion is not necessarily applicable to all highly shocked materials. The Martian shergottites experienced severe shocks, and yet their Zn isotopic compositions are fairly homogeneous (δ^{66}Zn = 0.13 - 0.35 ‰, Paniello et al., 2012b), and similar to those of most chondrites. This shows that post-shock heating is not always of sufficient intensity and duration to produce a detectable effect on the isotopic compositions of Zn, even in the case of shocked achondrites ejected during particularly energetic impacts.

A relationship between the shock levels and δ^{66}Zn was suggested with the first data obtained on ureilites (Moynier et al., 2010): apparently, the more severely a ureilite is shocked, the heavier its Zn isotopic composition is. ALH 81101, the most shocked sample that we analyzed here, displays the most extreme composition reported for a ureilite (δ^{66}Zn = 2.71 ‰), in agreement with this relationship. However, the strongly shocked GRA 95205, and the much less shocked GRO 95575, both display similar high δ^{66}Zn values (≈ 1.1 ‰), and suggest that impact processes were probably not the only reasons for the Zn isotopic heterogeneity of ureilites. Post-shock heating is difficult to estimate. Shock

pressures experienced by ureilites may not have exceeded 35 GPa (Bischoff et al., 1999). Therefore, post-shock reheating would be at most a few hundred degrees (Bischoff and Stöffler, 1992, Malavergne et al., 2001). Thus, it is questionable whether post-shock heating was sufficient to evaporate Zn and to fractionate its isotopes in these rocks.

To our knowledge, no experiment has attempted to evaluate the behavior of Zn by heating a peridotite under vacuum. However, several experiments using powders of ordinary chondrites were carried out at Purdue University at the end of the seventies (e.g., Ikramuddin et al., 1977a, 1977b). The behavior of Zn during the heating of ureilites and these materials must be fairly similar. These experiments show that no significant evaporation of Zn is detected in samples having been heated to less than 600°C for one week, but is substantial from 700°C (Fig. 6). Zn isotopes can be strongly fractionated during evaporation processes. Trinitite glasses produced during the first nuclear explosion (Day et al., 2017), and tektites (e.g., Moynier et al., 2009), for example, contain lower Zn abundances, and have heavier Zn isotopic compositions than their probable source materials, demonstrating the efficiency of these processes.

The breakup of the UPB was a particularly favorable context for evaporation of Zn. Indeed, at the time of its breakup, the mantle of the UPB was warm, as shown by the pre-breakup temperatures of the ureilites (> 1200 °C, e.g., Miyamoto et al., 1985). This hot mantle was covered by a trachyandesitic crust that was certainly much colder (Bischoff et al., 2014; Barrat et al., 2016b). The destruction of the body produced a multitude of fragments which have not all suffered the same shock levels. Mantle fragments were warm, and impact was probably only an additional heat-source which amplified the evaporation effects for the most shocked of them. Miyamoto et al. (1985, 1993) estimated the cooling rates of a few ureilites to be in the range of 1-6°C/hour. Assuming an initial temperature of 1250°C, and constant cooling rates, it can be estimated that less than a week to a month was required to cool ureilites down to 600°C, leaving sufficient time for evaporation processes.

The behavior of Zn during evaporation into a vacuum can be approximated using a Rayleigh distillation law:

$$\delta^{66}Zn_{final} = \delta^{66}Zn_{initial} + [(1000 + \delta^{66}Zn_{initial})(F^{(\alpha-1)} -1)] \quad (3)$$

where F is the fraction of Zn remaining in the rock, and $\delta^{66}Zn_{initial}$ and $\delta^{66}Zn_{final}$ are the $\delta^{66}Zn$ of the initial and final rocks, respectively. The value of α is difficult to estimate. In the case of trinitites, Day et al. (2017) have calculated apparent α values between 0.999 and 0.9995. Trinitites were melts, and the situation is certainly much more complex in the cases of solids or aggregates of crystals, where diffusion processes are necessarily involved (Moynier et al., 2010). In this study, we assumed an initial solid containing 300 µg/g of Zn with a $\delta^{66}Zn$ value equal to 0.5 ‰, and α values ranging from 0.993 to 1. The results of these calculations are shown in Figure 3. Although ureilites do not define a

unique trend in this diagram, the spread of the data can be explained by evaporation. Assuming initial concentrations were on the order of 300 µg/g, ureilites have lost up to 70 % of their Zn.

Fragments initially close to the surface of the body were rather cold. Post-shock heating was variable and not necessarily able to evaporate a significant fraction of their Zn. ALM-A, is one of these crustal samples. This lava is apparently not shocked (Bischoff et al., 2014). Therefore, this sample was not significantly reheated during the breakup of the body, and its Zn isotopic composition is probably pristine. As shown by terrestrial rocks, partial melting and fractional crystallization have only limited effects on the Zn isotopic composition of the least differentiated lavas (e.g., Chen et al., 2013; Sossi et al., 2018 among others). Because ALM-A is a primitive melt formed from a fertile source (Bischoff et al., 2014; Barrat et al., 2016), its Zn isotopic composition must be fairly close to the latter. Interestingly, its δ^{66}Zn (=0.67 ‰) is significantly higher than regular chondritic values. This observation has an important implication. It clearly shows that at least a portion of the UPB mantle already displayed high δ^{66}Zn values before the breakup of the body.

While there is no doubt that Zn isotopic compositions may have been substantially modified during the destruction of the body, we cannot exclude that the parent body had a heterogeneous mantle for Zn isotopes, similar to the heterogeneities in oxygen or carbon, for which a model involving two endmembers has been proposed (Barrat et al., 2017). The dispersion of the points observed in the δ^{66}Zn vs. olivine compositions plot (Fig. 4c) does not show a mixing curve, but does not exclude that such a relationship was present before the destruction of the parent body, with for example a ferroan endmember (A) having δ^{66}Zn values slightly heavier than those of the other endmember (B). This suggestion is at best speculative with the available data.

5. Conclusions

Including previous data (Moynier et al., 2010), ureilites display a wide range of δ^{66}Zn values, mainly from 0.40 to 1.26 ‰. ALH 81101, a strongly shocked ureilite extends this range to 2.71 ‰. These isotopic compositions are not correlated with the compositions of the olivine cores, nor with C and O isotopic compositions that are good recorders of the diversity of the materials which accreted to form the UPB. Moreover, our new analyses do not confirm the correlation between Zn abundances and δ^{66}Zn, nor the link between isotopic compositions and shock levels proposed by Moynier et al. (2010) with a more limited set of data. Nevertheless, and in line with the findings of the previous study, the wide range of Zn isotopic compositions shown by ureilites is certainly the result of evaporation processes. These processes more likely took place during the breakup of the UPB. Evaporation was possible because mantle temperatures were high at that time. In addition, post-shock heating certainly increased the losses of Zn of some ureilites, especially for the most shocked ones.

The Zn isotopic composition of the UPB before its destruction is an issue that has not yet been resolved. Despite a high number of meteorites, our sampling of the UPB is still too limited since we only have one "large" lava sample (ALM-A) and none of the core. New samples of ureilitic lavas or other crustal rocks, ideally unshocked, would be necessary to better constrain the UPB's composition before its breakup.

Acknowledgement

One of the ureilites from the Sahara was kindly provided by Bruno and Carine Fectay. Samples from Antarctica were kindly provided by the Meteorite Working Group (NASA) and the National Institute of Polar Research, Tokyo. US Antarctic meteorite samples are recovered by the Antarctic search for Meteorites (ANSMET) program which has been funded by NSF and NASA, and characterized and curated in the Department of Mineral Sciences of the Smithsonian Institution and Astromaterials Curation Office at NASA Johnson Space Center. Special thanks to Bryan Killingsworth and Richard Greenwood for the correction of the manuscript. We thank Qing-zhu Yin for the editorial handling, Paolo Sossi and two anonymous reviewers for their helpful and constructive reviews. This work was funded by a grant from the Programme National de Planétologie (CNRS-INSU) to JAB and by Conseil Général du Finistère for AA.

References

Barrat, J.A., Zanda, B., Moynier, F., Bollinger, C., Liorzou, C., and Bayon, G. (2012) Geochemistry of CI chondrites: Major and trace elements, and Cu and Zn isotopes. *Geochim. Cosmochim. Acta* **83**, 79-92.

Barrat, J. A., Rouxel, O., Wang, K., Moynier, F., Yamaguchi, A., Bischoff, A., Langlade, J. (2015) Early stages of core segregation recorded by Fe isotopes: insights from the ureilite meteorites. *Earth Planet. Sci. Lett.* **419**, 93–100.

Barrat, J. A., Dauphas N., Gillet, P., Bollinger, C., Etoubleau, J., Bischoff, A., Yamaguchi, A. (2016a) Evidence from Tm anomalies for non-CI refractory lithophile element proportions in terrestrial planets and achondrites. *Geochim. Cosmochim. Acta* **176**, 1-17.

Barrat, J.A., Jambon, A., Yamaguchi, A., Bischoff, A., Rouget, M.L., Liorzou, C. (2016b) Partial melting of a C-rich asteroid: Lithophile trace elements in ureilites. *Geochim. Cosmochim. Acta* **194**, 163-178.

Barrat, J.A., Sansjofre, P., Yamaguchi, A., Greenwood, R.C., Gillet, Ph. (2017) Carbon isotopic variation in ureilites: evidence for an early, volatile-rich Inner Solar System. *Earth Planet. Sci. Lett.* **478**, 143-149.

Bischoff A., Stöffler D. (1992) Shock metamorphism as a fundamental process in the evolution of planetary bodies; information from meteorites. *Eur. J. Mineral*. **4**, 707-755.

Bischoff A., Goodrich C. A., and Grund T. (1999) Shock-induced origin of diamonds in ureilites. Lunar Planet. Sci. XXX; # 1100, Lunar and Planetary Institute, Houston.

Bischoff, A., Horstmann, M., Pack, A., Laubenstein, M., Haberer, S., 2010. Asteroid 2008 TC_3—Almahata Sitta: A spectacular breccia containing many different ureilitic and chondritic lithologies. *Meteoritics & Planetary Science* **45**, 1638-1656.

Bischoff, A., Horstmann, M., Barrat, J. A., Chaussidon, M., Pack, A., Herwartz, D., Ward, D., Vollmer, C., Decker S. (2014) Trachyandesitic volcanism in the early Solar System. *Proc. Natl. Acad. Sci. U.S.A.* **111**(35), 12689–12692.

Bischoff A., Eber S., Patzek M., Horstmann M., Pack A., Decker S. (2016) Almahata Sitta news: well-known varieties and new species in the zoo. *Meteoritics Planet. Sci.* **51**, special issue, A167 (#6319, abstract).

Bridgestock L. J., Williams H., Rehkämper M., Larner F., Giscard M. D., Hammond S., Coles B., Andreasen R., Wood B. J., Theis K. J., Smith C. L., Benedix G. K. and Schönbächler M. (2014) Unlocking the zinc isotope systematics of iron meteorites. *Earth Planet. Sci. Lett.* **400**, 153–164.

Budde, G., Kruijer, T. S., Fischer-Gödde, M., Irving, A. J., Kleine, T. (2015) Planetesimal differentiation revealed by the Hf-W systematics of ureilites. *Earth Planet. Sci. Lett.* **430**,316-325.

Budde, G., Burckhardt, C., and Kleine, T. (2017) The distinct genetics of carbonaceous and non-carbonaceous meteorites inferred from molybdenum isotopes. 80th annual meeting of the Meteoritical Society, # 6271 (abstract).

Chikami J., Mikouchi T., Takeda H. and Miyamoto M. (1997) Mineralogy and cooling history of the calcium–aluminum–chromium-enriched ureilite Lewis Cliff 88774. *Meteorit. Planet. Sci.* **32**, 343-348.

Clayton, R. N. and Mayeda, T. K. (1988) Formation of ureilites by nebular processes. *Geochim. Cosmochim. Acta* **52**, 1313-1318.

Clayton, R. N. and Mayeda, T. K. (1996) Oxygen isotope studies of achondrites. *Geochim. Cosmochim. Acta* **69**, 1999–2017.

Day J. M. D., Moynier F., Meshik A. P., Pradivtseva O. V. Petit D. R. (2017) Evaporation fractionation of zinc during the first nuclear detonation. *Sci. Adv.* **3**, e1602668.

Doucet L. S., Mattielli N., Ionov D. A., Debouge W. and Golovin A. V. (2016) Zn isotopic heterogeneity in the mantle: a melting control? *Earth Planet. Sci. Lett.* **451**, 232–240.

Downes, H., Mittlefehldt, D. W., Kita, N. T. and Valley, J. W. (2008) Evidence from polymict ureilite meteorites for a disrupted and re-accreted single ureilite parent asteroid gardened by several distinct impactors. *Geochim. Cosmochim. Acta* **72**, 4825–4844.

Goodrich C. A. (1992) Ureilites: a critical review. *Meteoritics* **27**, 327-352.

Goodrich C. A., Scott E. R. D. and Fioretti A. M. (2004) Ureilitic breccias: clues to the petrologic structure and impact disruption of the ureilite parent asteroid. *Chem. Erde* **64**, 283-327.

Goodrich C. A., Van Orman J. A. and Wilson L. (2007) Fractional melting and smelting on the ureilite parent body. *Geochim. Cosmochim. Acta* **71**, 2876-2895.

Goodrich C. A., Hutcheon I. D., Kita N. T., Huss G. R., Cohen B. A. and Keil K. (2010) ^{53}Mn–^{53}Cr and ^{26}Al-^{26}Mg ages of a feldspathic lithology in polymict ureilites. *Earth Planet. Sci. Lett.* **295**, 531–540.

Goodrich C. A., Ash R. D., Van Orman J. A., Domanik K. and McDonough W. F. (2013) Metallic phases and siderophile elements in main group ureilites: implications for ureilite petrogenesis. *Geochim. Cosmochim. Acta* **112**, 340–373.

Goodrich C. A., Bischoff A., and O'Brien D. P. (2014a). Asteroid 2008 TC_3 and the fall of Almahata Sitta, a unique meteorite breccia. *Elements* 10, 31-37.

Goodrich C.A., Harlow G.E., Van Orman J.A., Sutton S.R., Jercinovic M.J., Mikouchi T. (2014b) Petrology of chromite in ureilites: deconvolution of primary oxidation states and secondary reduction processes. *Geochim. Cosmochim. Acta* **135**, 126-169.

Goodrich, C.A., Hartmann, W.K., O'Brien, D., Weidenschilling, S.J., Wilson, L., Michel, P., Jutzi, M., (2015) Origin and history of ureilitic material in the solar system: the view from asteroid 2008 TC3 and the Almahata Sitta meteorite. *Meteorit. Planet. Sci.* **50**, 782–809.

Horstmann M. and Bischoff A. (2014) The Almahata Sitta polymict breccia and the late accretion of Asteroid 2008 TC_3 - Invited Review. *Chemie der Erde - Geochemistry* **74**, 149-184.

Huang, J., Chen, S., Zhang, X.-C., & Huang, F. (2018). Effects of melt percolation on Zn isotope heterogeneity in the mantle: Constraints from peridotite massifs in Ivrea-Verbano Zone, Italian Alps. *J. Geophys. Res.: Solid Earth*, **123**, 2706–2722.

Ikramuddin M., Binz C.M., Lipschutz M.E. (1977a) Thermal metamorphism of primitive meteorites - III. Ten trace elements in Krymka L3 chondrite heated at 400–1000°C. *Geochim. Cosmochim. Acta* **41**, 393-401.

Ikramuddin M., Matza S. and Lipschutz M. E. (1977b) Thermal metamorphism of primitive meteorites - V. Ten trace elements in Tieschitz H3 chondrite heated at 400–1000°C. *Geochim. Cosmochim. Acta* **41**, 1247–1256.

Le Roux, V., Dasgupta, R., Lee, C. T. A. (2011) Mineralogical heterogeneities in the Earth's mantle: constraints from Mn, Co, Ni and Zn partitioning during partial melting. *Earth Planet. Sci. Lett*. **307**, 395-408.

Luck J. M., Ben Othman D. and Albarède F. (2005) Zn and Cu isotopic variations in chondrites and iron meteorites: early solar nebula reservoirs and parent-body processes. *Geochim. Cosmochim. Acta* **69**, 5351-5363.

Lodders K. (2003) Solar system abundances and condensation temperatures of the elements. *Astrophys. J.* **591**, 1220–1247.

Maréchal C., Telouk P. and Albarède F. (1999) Precise analysis of copper and zinc isotopic compositions by plasma-source mass spectrometry. *Chem. Geol.* **156**, 251–273.

Mahan B., Siebert J., Pringle E. A. and Moynier F. (2017) Elemental partitioning and isotopic fractionation of Zn between metal and silicate and geochemical estimation of the S content of the Earth's core. *Geochim. Cosmochim. Acta* **196**, 252–270.

Mahan B., Moynier F., Beck P., Pringle E.A., Siebert J. (2018) A history of violence: insights into post-accretionary heating in carbonaceous chondrites from volatile element abundances, Zn isotopes and water contents. *Geochim. Cosmochim. Acta* **220**, 19-35.

Malavergne V., Guyot F., Benzerara K. and Martinez I. (2001) Description of new shock-induced phases in the Shergotty, Zagami, Nakhla and Chassigny meteorites. *Meteorit. Planet. Sci.* **36**, 1297-1305.

Mittlefehldt D. W., McCoy T. J., Goodrich C. A. and Kracher A. (1998) Non-chondritic meteorites from asteroidal bodies. In Planetary Materials (ed. J. J. Papike). Mineralogical Society of America, Washington, DC, p. 195.

Miyamoto, M., Takeda, H., Toyoda H. (1985) Cooling history of some Antarctic ureilites. *J. Geophys. Res.* **90** (supplement), D116–D122.

Miyamoto, M., Furuta, T., Fujii, N., McKay D.S., Lofgren G.E., Duke, M.B. (1993) The Mn-Fe negative correlation in olivines in ALHA 77257 ureilite. *J. Geophys. Res.* **98**, E3, 5301-5307.

Morbidelli A., Lunine J.I, O'Brien D.P., Raymond S.N., Walsh K.J. (2012) Building terrestrial planets. *Annu. Rev. Earth Planet. Sci.* **40**, 251-275.

Moynier F., Beck P., Jourdan F., Yin Q.-Z., Reimold U. and Koeberl C. (2009) Isotopic fractionation of Zn in tektites. *Earth Planet. Sci. Lett.* **277**, 482–489.

Moynier F., Beck P., Yin Q.Z., Ferroir T., Barrat J.A., Paniello R., Telouk P., Gillet P. (2010) Volatilization induced by impacts recorded in Zn isotope composition of ureilites. *Chem. Geol.* **276**, 374-379.

Moynier F., Paniello R. C., Gounelle M., Albarède F., Beck P., Podosek F. and Zanda B. (2011) Nature of volatile depletion and genetic relationships in enstatite chondrite and aubrites inferred from Zn isotopes. *Geochim. Cosmochim. Acta* **75**, 297-307.

Nabiei F., Badro J., Dennenwaldt T., Oveisi E., Cantoni M., Hébert C., El Goresy A., Barrat J.A., Gillet Ph. (2018) A large planetary body inferred from diamond inclusions in a ureilite meteorite. *Nature Comm.*, DOI :10.1038/s41467-018-03808-6.

O'Neill H. St. C. and Palme H. (2008) Collisional erosion and the non-chondritic composition of the terrestrial planets. *Phil. Trans. R. Soc.* A **366**, 4205-4238.

Paniello R.C., Moynier F., Beck P., Barrat J.A., Podosek F.A., Pichat S. (2012a) Zinc isotopes in HEDs: clues to the formation of 4-Vesta, and the unique composition of PCA 82502. *Geochim. Cosmochim Acta.* **86**, 76-87.

Paniello R., Day J. M. D. and Moynier F. (2012b) Zinc isotopic evidence for the origin of the Moon. *Nature* **490**, 376–380.

Pringle E.A., Moynier F., Beck P., Paniello R., Hezel D.C. (2017) The origin of volatile element depletion in early solar system material: clues from Zn isotopes in chondrules. *Earth Planet. Sci. Lett.* **468**, 62-71.

Rosén Å.V., Pape J., Hofmann B.A., Gnos E., Guillong M. (2019) Quenched primary melt in Ramlat as Sahmah 517 – Snapshot of ureilite anatexis in the early solar system, *Geochim. Cosmochim. Acta*, doi: https://doi.org/10.1016/j.gca.2018.11.016 (in press).

Rankenburg K., Humayun M., Brandon A. D., Herrin J.S. (2008) Highly siderophile elements in ureilites. *Geochim. Cosmochim. Acta* **72**, 4642–4659.

Rubin A. E., Huber H. and Wasson J. T. (2009) Possible impact induced refractory-lithophile fractionations in EL chondrites. *Geochim. Cosmochim. Acta* **73**, 1523–1537.

Sanders, I.S., Scott, E.R.D., Delaney J.S. (2017) Origin of mass-independent oxygen isotope variation among ureilites: Clues from chondrites and primitive achondrites. *Meteoritics Planetary Sci.* **52**, 690-708.

Scott, E. R. D., Taylor, G. J., Keil, K. (1993) Origin of ureilite meteorites and implications for planetary accretion. *Geophys. Res. Lett.* **20**, 415-418.

Singletary, S.J., Grove, T.L. (2003) Early petrologic processes on the ureilite parent body. *Meteoritics Planet. Sci.* **39**, 95-108.

Sossi P.A., Nebel O., O'Neil H. St. C., Moynier F. (2018) Zinc isotope composition of the Earth and its behaviour during planetary accretion. *Chem. Geol.* **477**, 73-84.

Sossi, PA, Halverson, GP, Nebel, O, Eggins, SM (2015) Combined separation of Cu, Fe and Zn from rock matrices and improved analytical protocols for stable isotope determination. *Geostand Geoanaly Res* **39**, 129-149.

Takeda H. (1987) Mineralogy of Antarctic ureilites and a working hypothesis for their origin and evolution. *Earth Planet. Sci. Lett.* **81**, 358–370.

Van Kooten E.M.M.E., Schiller M., Bizzarro M. (2017) Magnesium and chromium isotope evidence for initial melting by radioactive decay of ^{26}Al and late impact-melting of the ureilite parent body. *Geochim. Cosmochim. Acta* **208**, 1-23.

Wang Z. Z., Liu S. A., Liu J., Huang J., Xiao Y., Chu Z. Y., Zhao X. M., Tang L. (2017) Zinc isotope fractionation during mantle melting and constraints on the Zn isotope composition of Earth's upper mantle. Geochim. Cosmochim. Acta 198, 151-167.

Warren, P. H. (2011) Stable isotopes and the noncarbonaceous derivation of ureilites, in common with nearly all differentiated planetary materials. *Geochim. Cosmochim. Acta* **75**, 6912-6926.

Warren, P.H. (2012) Parent body depth–pressure–temperature relationships and the style of the ureilite anatexis. *Meteoritics Planet. Sci.* **47**, 209-227.

Warren, P.H., Huber, H. (2006) Ureilite petrogenesis: A limited role for smelting during anatexis and catastrophic disruption. *Meteoritics Planet. Sci.* **41**, 835-849.

Warren P. H. and Kallemeyn G. W. (1992) Explosive volcanism and the graphite-oxygen fugacity buffer on the parent asteroid (s) of the ureilite meteorites. *Icarus* **100**, 110–126.

Warren, P.H., Ulff-Møller, F., Huber, H., Kallemeyn, G.W. (2006) Siderophile geochemistry of ureilites: A record of early stages of planetesimal core formation. *Geochim. Cosmochim. Acta* **70**, 2104-2126.

Wasson J. T. and Kallemeyn G. W. (1988) Compositions of chondrites. *Philos. Trans. R. Soc. London*, **A325**, 535–544.

Wilson L., Goodrich C.A., Van Orman J.A. (2008) Thermal evolution and physics of melt extraction on the ureilite parent body. *Geochim. Cosmochim. Acta* **72**, 6154-6176.

Wulf A.V., Palme H., Jochum K.P. (1995) Fractionation of volatile elements in the early solar system: evidence from heating experiments on primitive meteorites. *Planet. Space Sci.* **43**, 451-468.

Yamaguchi A., Barrat J.A., Greenwood R.C. (2017). Achondrites. Encyclopedia of Geochemistry, White W.M. (ed), Springer International Publishing AG, DOI 10.1007/978-3-319-39193-9_303-1.

Yin Q., Jacobsen S. B., Yamashita K., Blichert-Toft J., Te´louk P., and Albarède F. (2002) A short timescale for terrestrial planet formation from Hf-W chronometry of meteorites. *Nature* **418,** 949–952.

Table 1. Details of ureilite samples studied, shock level (L: low, M: medium, H: high, Goodrich, 1992), olivine core compositions (Singletary and Grove, 2003; Downes et al., 2008; Barrat et al., 2015 and reference therein), Ca, Mn and Zn abundances (Bischoff et al., 2014; Barrat et al., 2016b and this work), and Zn isotopic compositions (errors given here are calculated from the difference between the duplicates). Source abbreviations are: MWG= NASA meteorite working group; NIPR= National Institute of Polar Research, Tokyo; UBO= Université de Bretagne Occidentale, Brest.

	source	split	shock	Fo%	CaO (wt%)	Mn (µg/g)	Zn (µg/g)	$\delta^{66}Zn_{IRMM3702}$	$\delta^{68}Zn_{IRMM3702}$	$\delta^{66}Zn_{Lyon}$
Antarctic finds										
A 881931	NIPR	,71	L	78.7	1.52	3103	240	0.364±0.003	0.905±0.022	0.66
ALH 77257	NIPR	,105	L	86.1	0.90	3005	204	0.474±0.006	1.002±0.020	0.77
ALH 81101	MWG	,63	H	78.9	1.08	2593	114	2.409±0.009	4.861±0.011	2.71
ALH 82130	MWG	,43	L	95.2	2.62	3171	180	0.519±0.002	1.116±0.008	0.82
EET 83225	MWG	,37	M?	88.3	2.32	3306	99	0.319±0.005	0.774±0.001	0.62
EET 96042	MWG	,48		81.3	1.34	2713	221	0.381±0.003	0.800±0.025	0.68
GRA 95205	MWG	,64	H	79.2	0.64	2607	154	0.852±0.006	1.874±0.029	1.15
GRO 95575	MWG	,46	L	78.6	1.31	2828	130	0.809±0.004	1.615±0.044	1.11
LAP 03587	MWG	,10	M	74.7	0.71	3075	238	0.337±0.015	0.785±0.018	0.64
LAR 04315	MWG	,46	H	81.9	1.69	2940	161	0.961±0.013	1.975±0.042	1.26
MET 78008	NIPR	,69	M	75.9	2.43	2711	*285*	0.609±0.012	1.309±0.008	0.91
MET 01085	MWG	,23		88.8^{px}	2.23	3230	89	0.390±0.007	0.803±0.020	0.69
PCA 82506	MWG	,125	L	79.2	1.06	2648	170	0.393±0.010	0.914±0.038	0.69
Y 74130	NIPR	,55	LM	77.0	1.48	2831	*196*	0.588±0.007	1.241±0.033	0.89
Y 790981	NIPR	,85	M	77.5	1.09	3105	252	0.658±0.004	1.347±0.012	0.96
Y 791538	NIPR	,109	L	91.3	1.65	3009	228	0.268±0.001	0.612±0.023	0.57
Y 980110	NIPR	,56	M	88.2	1.75	2890	103	0.707±0.022	1.523±0.044	1.01
Y 981810	NIPR	,76	L	78.3	1.19	2831	227	0.494±0.019	1.058±0.019	0.79

Table 1 (continue)

	source	split	shock	Fo%	CaO (wt%)	Mn (µg/g)	Zn (µg/g)	$\delta^{66}Zn_{IRMM3702}$	$\delta^{68}Zn_{IRMM3702}$	$\delta^{66}Zn_{Lyon}$
Hot desert finds										
NWA 2234	NIPR		L	81.5	1.74	2460	122	0.560±0.001	1.285±0.002	0.86
NWA 2236	NIPR		L	96.8	2.21	2815	212	0.313±0.002	0.736±0.032	0.61
NWA 5884	Barrat		L	78.6	0.80	2784	212	0.441±0.001	0.924±0.038	0.74
NWA 6056	Barrat		M	84.8	1.41	3176	210	0.412±0.004	0.881±0.010	0.71
NWA 7630	Barrat			79.1	1.13	2689	188	0.275±0.005	0.611±0.008	0.58
NWA 7686	Barrat			91.0	1.30	2848	236	0.387±0.013	0.870±0.010	0.69
NWA 8049	Barrat			84.3	1.16	2891	199	0.442±0.006	0.909±0.001	0.74
NWA 11372	UBO		H	77.8	1.26	2746	140	0.648±0.007	1.369±0.004	0.95
Almahata Sitta										
ALM-A	Münster				7.29	2090	148	0.371±0.009	0.779±0.023	0.67
Standard										
BHVO-2 (n=8)								0.034 (σ=0.019)	0.078 (σ=0.035)	0.33

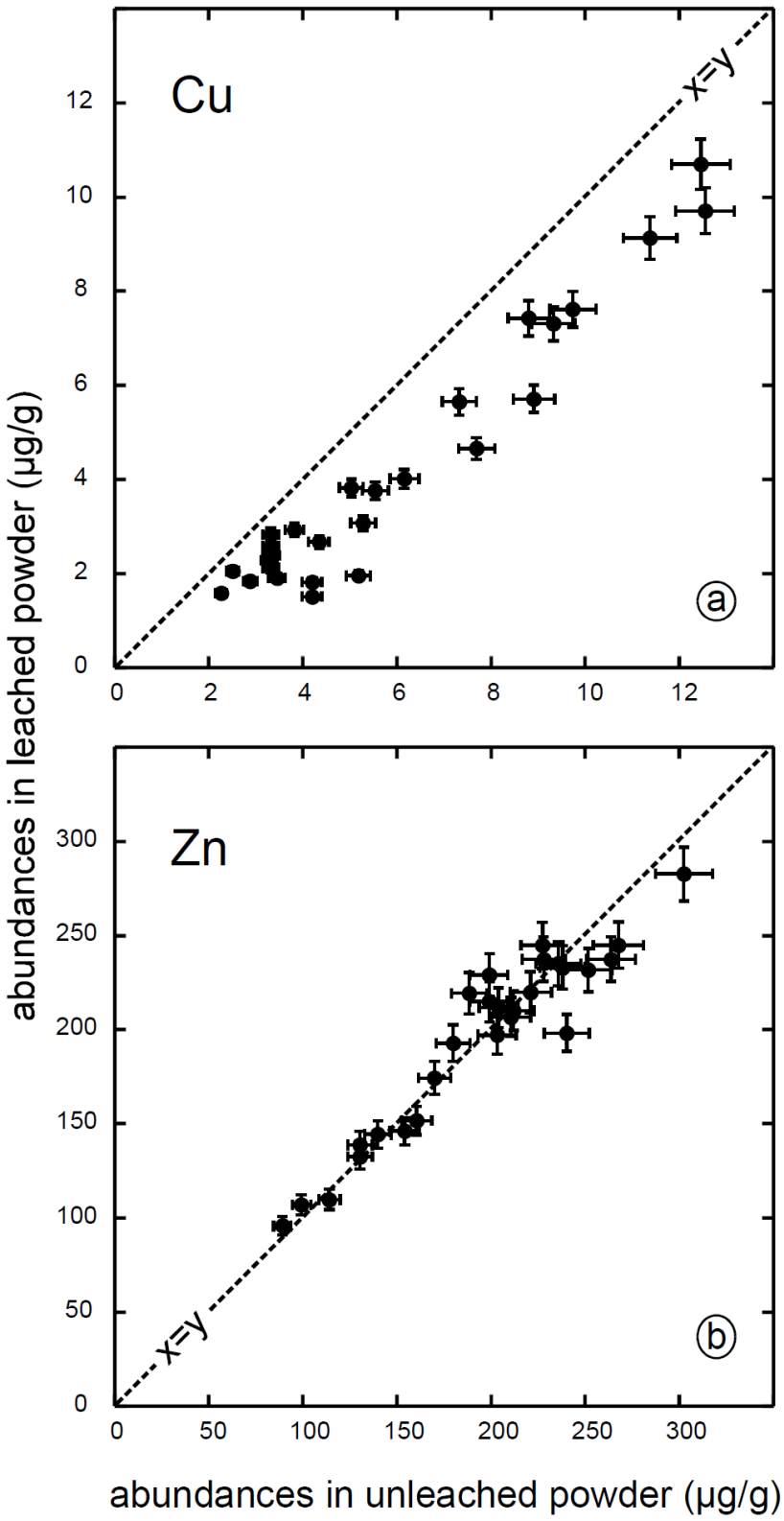

Fig. 1. Cu (a) and Zn (b) abundances in the residues compared to the same abundances in the unleached powders prepared with chips of ureilites (Barrat et al., 2016b). Residues were obtained after leaching the powder 30 minutes in 4 N HNO_3 at room temperature (see Barrat et al., 2016b for more details). The error bars are 2 σ confidence intervals.

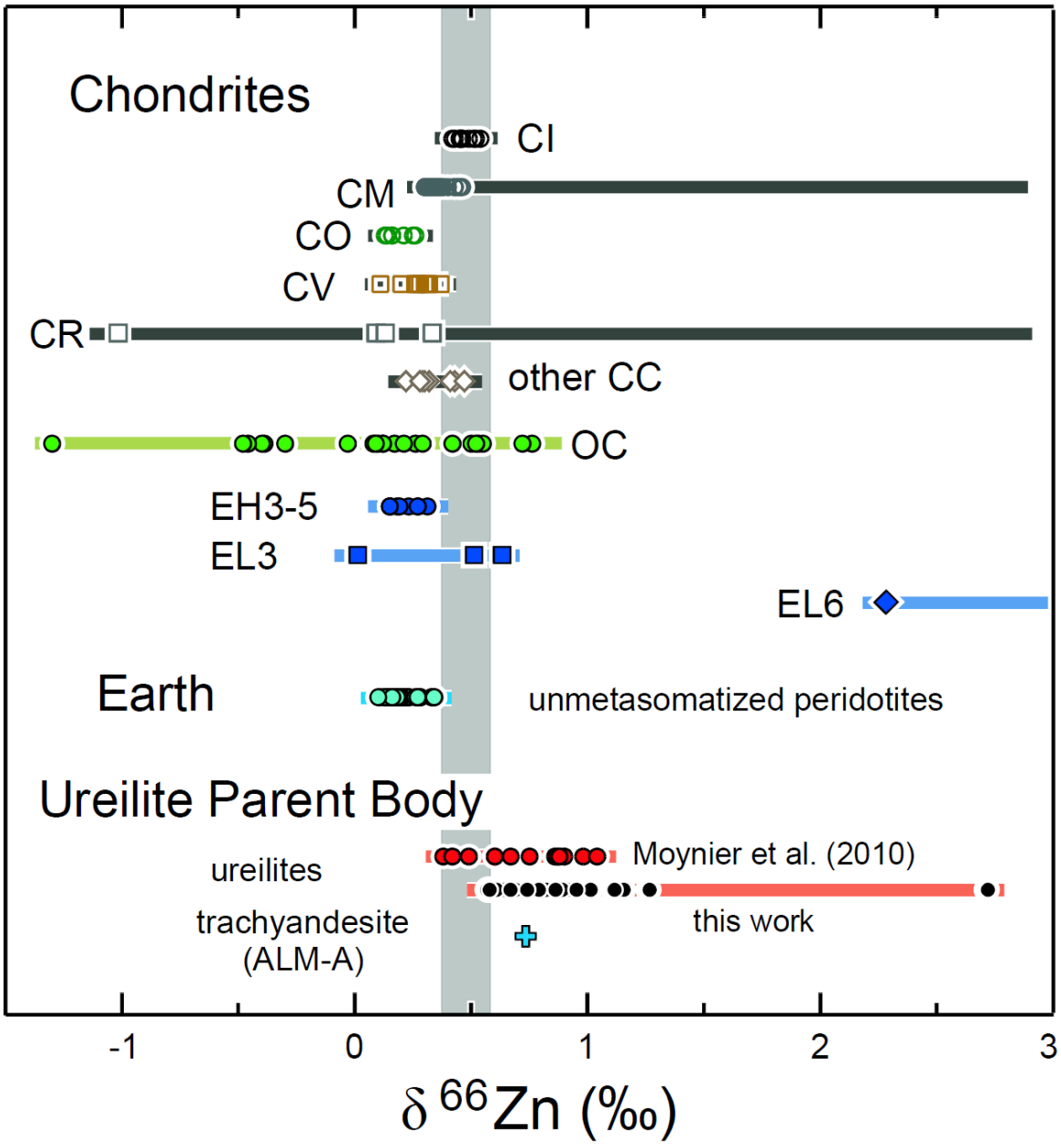

Fig. 2. Compilation of available Zn isotopic data for chondrites, terrestrial peridotites and ureilitic meteorites. The grey vertical band represents the δ^{66}Zn range of CI chondrites. Chondrite data are from Luck et al. (2005), Moynier et al. (2011), Barrat et al. (2012), Pringle et al. (2017), and Mahan et al. (2018). Peridotite data are from Doucet et al. (2016),Wang et al. (2017), Huang et al. (2018) and Sossi et al. (2018).

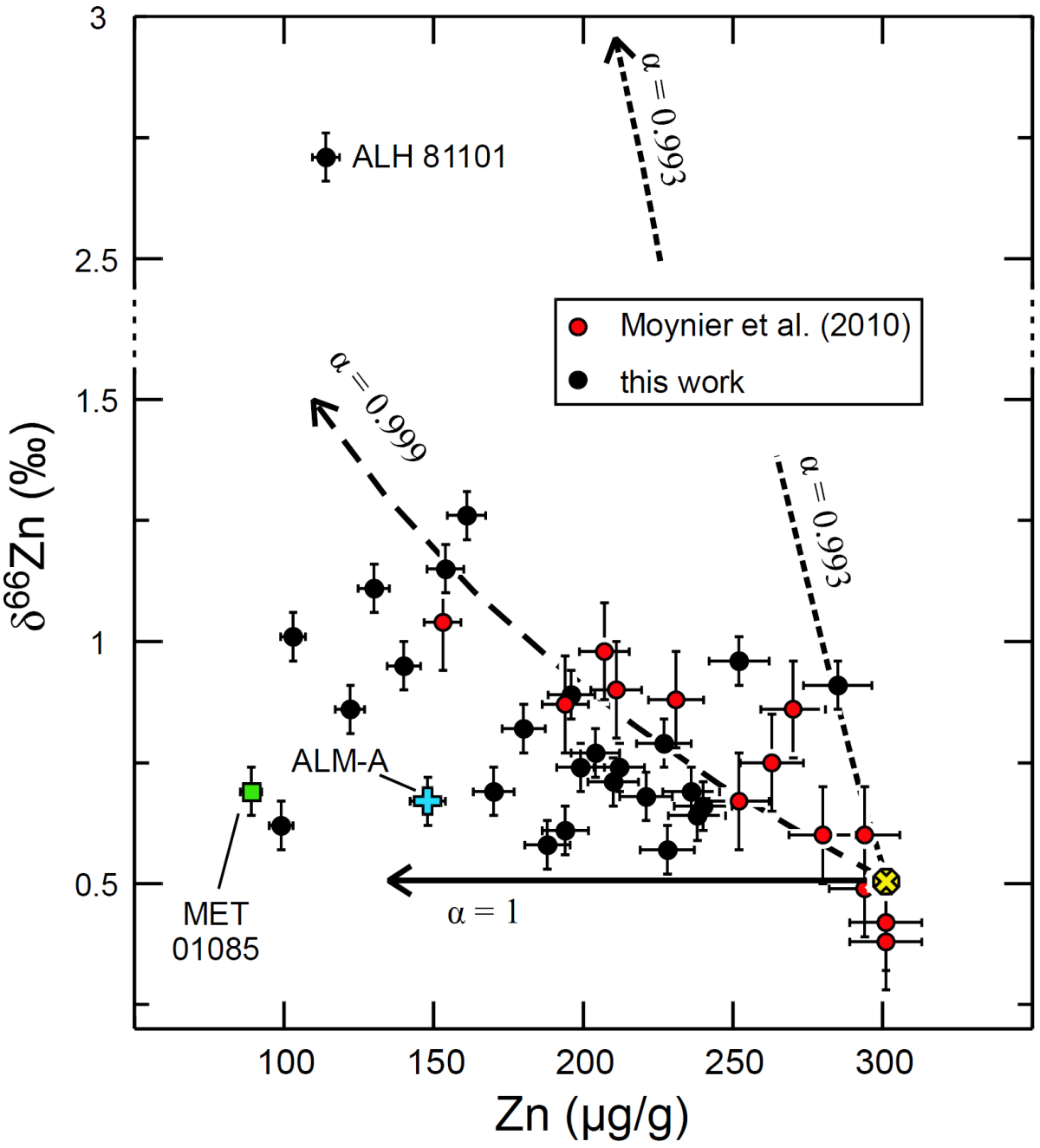

Fig. 3. δ^{66}Zn vs. Zn abundances in ureilites. The error bars are 2 σ confidence intervals. Trends for Zn evaporation for a material containing 300 µg/g of Zn, are drawn for three different α values using a Rayleigh distillation law (see the text for more details).

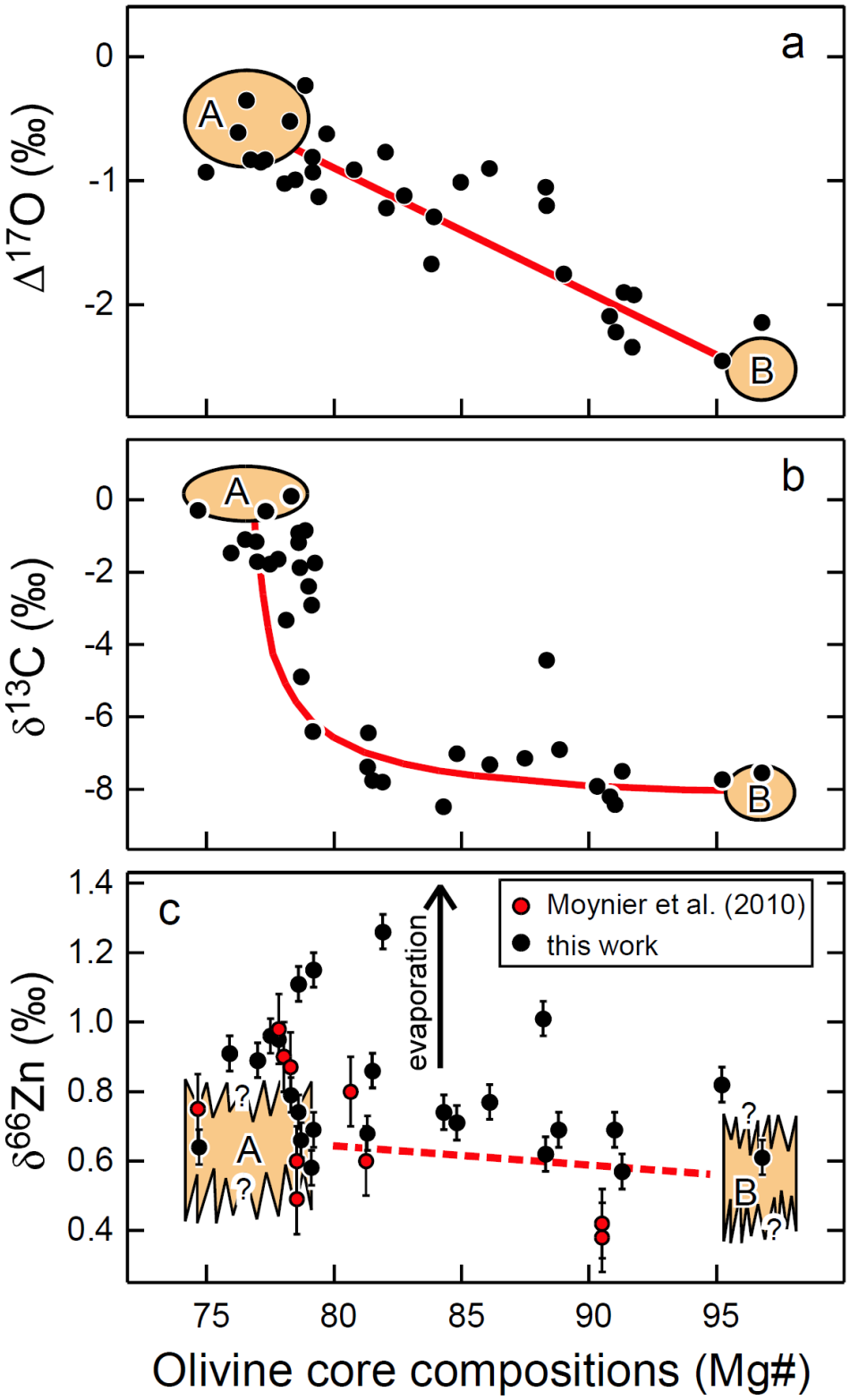

Fig. 4. $\Delta^{17}O$ (a), $\delta^{13}C$ (b), $\delta^{66}Zn$ (c) vs. olivine core compositions (Mg#) from unbrecciated ureilites. Oxygen isotopic compositions and $\delta^{13}C$ are from Clayton and Mayeda (1996) and Barrat et al. (2017) respectively. O and C isotopic compositions indicate that the ureilite compositions are well explained by a mixing of two components. Mixing lines and curves between A and B, the two endmembers, are drawn in red. The error bars are 2 σ confidence intervals. When not drawn, the errors are equivalent to the size of the data points.

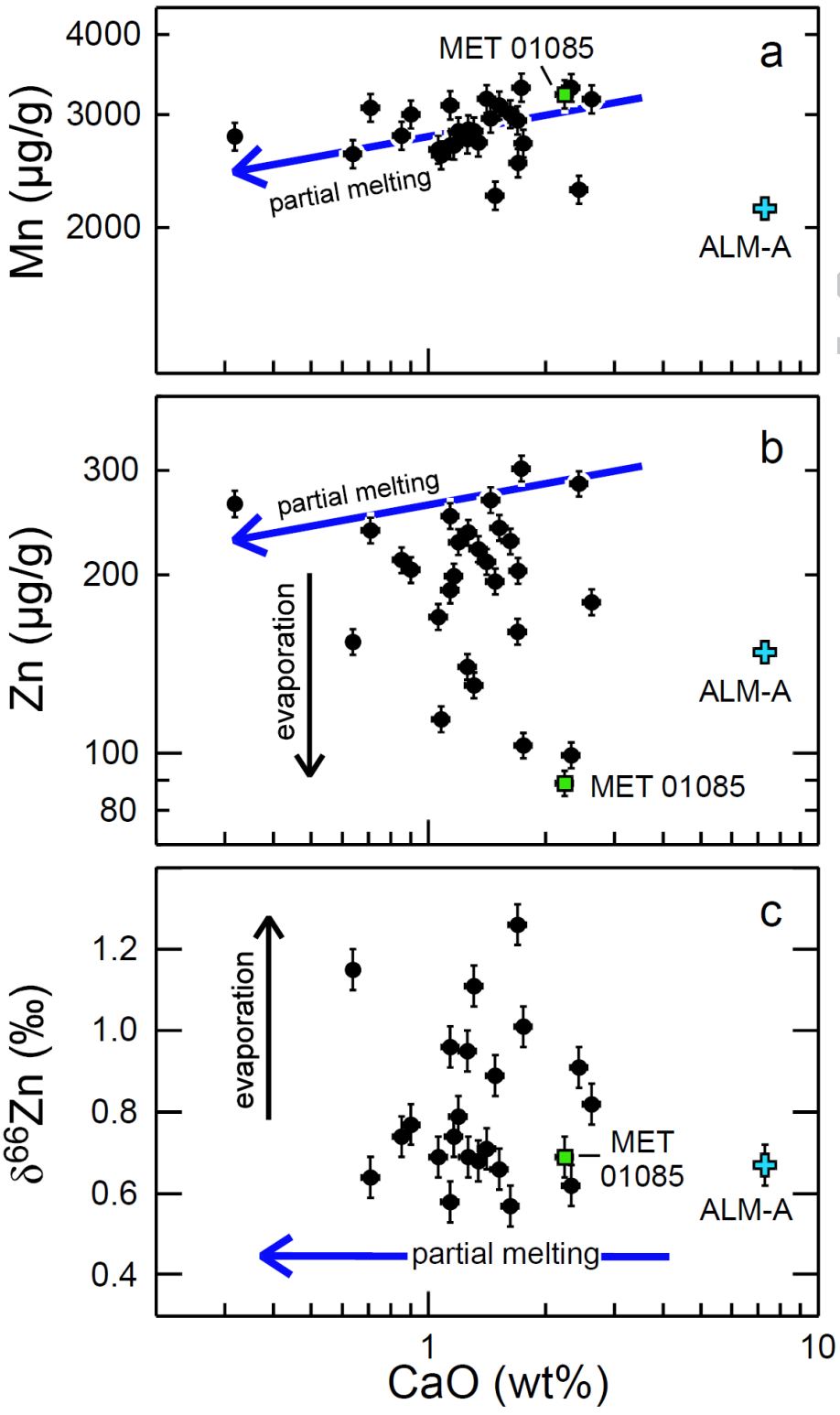

Fig. 5. Mn (a), Zn (b) and δ^{66}Zn (c) vs. CaO abundances in ureilites. The error bars are 2 σ confidence intervals.

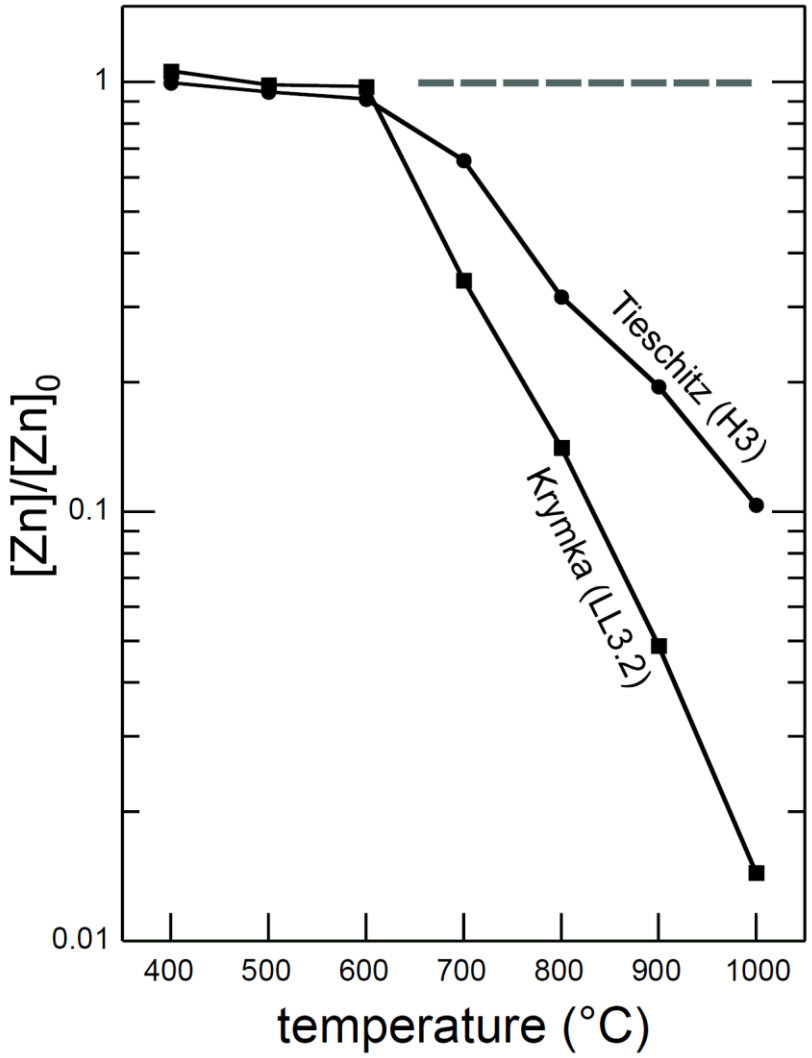

Fig. 6. Behavior of Zn during the heating of powders prepared with two ordinary chondrites. Samples were heated during one week under vacuum (≈10^{-5} atm H_2) at different temperatures (Ikramuddin et al., 1977a, 1977b).